MET.O.14

METEOROLOGICAL OFFICE
BOUNDARY LAYER RESEARCH BRANCH
TURBULENCE & DIFFUSION NOTE

T.D.N. No. 70

(up-dated version)

BOUNDARY LAYER TURBULENCE SPECTRA IN STABLE CONDITIONS

by

S.J. Caughey

January 1976

BOUNDARY LAYER TURBULENCE SPECTRA IN STABLE CONDITIONS

by

S J Caughey

Meteorological Research Unit, R A F Cardington, Bedford, England.

Abstract:-

Simultaneous measurements of horizontal wind speed, vertical wind speed and temperature fluctuations at heights up to 91 m in the stable atmospheric boundary layer are described. The power and cospectral shapes show a low frequency peak (near the Brunt-Vaisala frequency) separated by a spectral gap from a peak at high frequency due to turbulence. Spectral shapes in the turbulence subrange at 8 m are in good agreement with the universal curves previously presented by Kaimal (1973). Further information is given on the variation of the scaling parameter, f_o, with stability and the applicability of the normalising procedure to the spectra from the higher levels is discussed.

BOUNDARY LAYER TURBULENCE SPECTRA IN STABLE CONDITIONS

by

S J Caughey

1. Introduction:-

In some recent papers (Kaimal et al (1972), Kaimal (1973)) the spectral characteristics of surface layer turbulence in stable conditions over a flat, uniform site in Kansas (see Haugen et al, 1970) were investigated. When properly nondimensionalized all the spectra/cospectra (at heights up to 22.6 m) could be represented by a set of universal curves. The technique used is based on applying a low frequency cut-off to the data, to hopefully eliminate the influence of low frequency oscillations and trends in the time series. Kaimal chose a cut-off frequency at .005 Hz and then by integrating the spectra/cospectra over greater frequencies obtained new variances/covariances ($\overline{\alpha^2}$ / $\overline{\alpha\beta}$) relevant to the turbulence region. This paper presents data which clearly demonstrates the existence of a spectral gap near .008 Hz ie close to the low frequency cut-off chosen by Kaimal. The variation of this gap with height is also described.

The collapse of the spectra into universal curves was achieved by introducing a new scaling parameter (f_o) which is the intercept on a reduced frequency scale (f, $= \frac{nZ}{u}$) at which the extrapolated inertial subrange slope meets the line $\frac{n S_\alpha(n)}{\overline{\alpha^2}} = 1$ (or $\frac{n C_{\alpha\beta}(n)}{\overline{\alpha\beta}}$ = 1, for cospectra). Plots of the nondimensionalized spectra/cospectra were then found to be universal functions of f/f_o. Although $f/f_o = n/n_o$, f/f_o is used since n_o varies with height. Kaimal has shown that f_o ($= Z/\lambda_o$, where λ_o is the equivalent spatial scale) is independent of height and varies linearly with Richardson number (Ri) (but in a more complicated way with Z/L). This linear dependence on Ri greatly enhances the usefulness of the normalisation since from relatively simple measurements of wind and temperature profiles one can determine the spectral characteristics of surface layer turbulence in a wide range of stabilities.

Earlier results from measurements in stable conditions by McBean (1971) indicated considerable scatter in the spectral estimates for $f < .1$, to the extent that for the horizontal wind speed spectra no meaningful average line could be drawn. Furthermore Busch (1973) found that unavoidable effects from nonstationarity and large scale inhomogeneities set a lower frequency limit below which Monin-Obukhov similarity did not appear to hold. Because of the almost ideal nature of the Kansas site it is important to establish the applicability of the results to the more usual (ie much more inhomogeneous and rough) site typical of micrometeorological work. This paper discusses a series of spectra/cospectra obtained at Cardington, England (the site consists of 100 metres square of short grass set in typical agricultural/rural countryside). Some information is given on special shapes at heights up to 91 m and the behaviour of the low frequency spectral regions is discussed in terms of the Brunt-Vaisala frequency.

The data were obtained using three-component Cardington turbulence probes (see Readings and Butler, (1972)) which measured the instantaneous values of the temperature (T), the total wind speed (V) and the inclination of the flow to the horizontal plane (Ø) at 91 m (on a balloon cable), 46 m (on a tower) and 8 m (on a mast). Each variable was sampled once/second, setting an upper frequency limit to the spectra of about 0.5 Hz. The spectral analysis was carried out using a fast Fourier Transform (see Rayment, (1970)). Profiles of mean wind speed and temperature up to 16 m were recorded every two minutes. These were supplemented with profiles of wind speed, temperature and humidity to several hundred metres from the Cardington Balthum (Painter, (1970)). The data set from which the results are drawn comprises two multilevel runs of about 5 hours and 6 hours duration on the 8/9 November 1972 and 10/11 January 1973 respectively.

2. Spectral results at low frequency:-

The data to be discussed here were obtained on the night 8/9 November 1972 between 2300 GMT and 0415 GMT. Throughout this period the Balthum ascents showed a $5^{o}K$ nocturnal inversion extending from the surface to about 200 m.

Overall spectra for the quantities U, W and T (ie horizontal wind speed, vertical wind speed and temperature fluctuations respectively) for the three heights are shown in Fig 1 (a), (b) and (c), plotted in the form $n\,S(n)$ versus f. Several points of interest emerge,

i. A spectral gap is clearly discernible on the U and T spectra (at 8 m) near f $\sim$ .02 (Corresponding to a natural frequency near .008 Hz) and at this frequency the fall off in the W component spectrum (varying as n^{+1}) is arrested.

ii. It is to be expected that the local value of the Brunt-Vaisala frequency (N), where

$$N = \frac{1}{2\pi}\sqrt{\frac{g}{\Theta_v}\frac{d\Theta_v}{dz}} \qquad (1)$$

(Θ_v is the virtual potential temperature)

will set an upper limit to the frequencies of any waves present (see Gossard et al 1971, Caughey and Readings, 1975). Values of N at the three heights are given in Table 1 (these were found to be nearly constant across the period of observation). The peak at low frequency (near f= .002, see Fig (1)) is in the neighbourhood of the Brunt-Vaisala frequency and in line with the latter moves to higher reduced frequencies with increasing height. It cannot be expected that the Brunt-Vaisala frequency will give any more than a rough indication of the position of this peak since the observed frequencies of any waves present will have been Doppler shifted by the mean flow.

iii. The W component probably most clearly reflects the presence of waves (or other low frequency contributions) and Fig 1 (b) indicates that the contributions from these becomes more important with increasing height. The importance of waves would be expected to vary from one occasion to another and in section 3 an example is given in which the contribution is small.

iv. The cospectral peaks at low frequency (ie those for $\overline{WT}$, $\overline{UW}$ and $\overline{UT}$) also occurred in the vicinity of the Brunt-Vaisala frequency however a phase and coherence spectral analysis (see eg Caughey and Readings, 1975) did not provide conclusive evidence of the presence of waves.

3. <u>Spectral characteristics of the turbulence subrange</u>:-

To obtain the variances/covariances for the turbulent region Kaimal (1973) integrated the spectral estimates over the frequency band $.005 < n < 10$ Hz. This lower frequency limit was found to be somewhat low for the present data. Shown in Fig (2) are temperature spectra typical of the periods when the turbulence was continuous at heights of 8, 46 and 91m (for the complete data set the turbulence, at 8 m, was classified as continuous about 60% of the time, sporadic 20% and weak for 20%). At the lowest height two peaks are apparent separated by a gap centred near .008 Hz. Furthermore the turbulence spectrum (ie frequencies $>$ .008 Hz) exhibits the expected features ie a roll off at low frequencies (slope $\approx n^{+1}$) and a high frequency decline near $n^{-\frac{2}{3}}$. At 46m a spectral gap is still discernable however the separation of the two peaks has decreased significantly because the turbulence spectrum has shifted to lower frequencies. The spectrum at 91m shows the gap essentially unresolved with the spectrum now assuming a single peaked character. It is worth noting that at this and greater heights where the fluctuations due to turbulence and wave motion (or low frequency trends) fall in similar frequency bands then techniques such as phase and coherence spectral analysis will not prove useful in distinguishing between the two. To compare the turbulence spectra with the universal curves from Kaimal (1973) the variances have been obtained by integrating over the frequency band $.008 < n < .5$Hz.

The spectral results for temperature and horizontal wind speed at 8m are shown in Fig 3 (a) and (b) (a similar comparison for the vertical velocity component at 8m could not be carried out because the sampling rate was inadequate to clearly resolve the spectral peak, see Fig 1(b). A good approximation to both spectral shapes is obtained with the relationship,

$$\frac{n S_{\alpha}(n)}{\overline{\alpha^2}} = \frac{A(f/f_0)}{1 + A(f/f_0)^{5/3}} \qquad (2)$$

where α = u or T

and A = 0.3

This is in good agreement with the line from Kaimal (1973) (ie A = .164, shown dashed on Fig 3). The difference between the A values is almost certainly accounted for by the different frequency bands over which the variances have been computed ie the best fit A value will depend on the lower frequency limit (chosen somewhat subjectively) and the upper limit set by the sampling rate.

The relationships between f_o (for horizontal wind and temperature) and Richardson number (Ri) for 12 thirty-five minute runs at 8m (4 from 8/9 Nov. and 8 from 10/11 Jan.) are given in Fig 4 (a) and (b) (Ri values were obtained by fitting polynomials in lnZ to the potential temperature and wind speed profiles). Since $f_o = Z/\lambda_o$, where λ_o is the equivalent spatial scale and Z = 8m this figure essentially shows the variation of λ_o with stability (Ri). Good agreement with Kaimal's (1973) relationships (dashed lines) is indicated, the best fit lines being,

$$(f_o)_T = .74Ri + .0013$$
$$(f_o)_u = .53Ri - .0033 \qquad .005 < Ri < .1$$

It is important to note that the Ri values for this data extend to a decade lower (.005) than those in Kaimal's data ie combining both sets of results it can be stated that the proportionality between $(f_o)_T$ and $(f_o)_u$ and Ri is now established over the range $.005 < Ri < .2$. These results indicate that, at 8m, the charateristic scale for temperature fluctuations $(\lambda_o)_T$ reduces from 0.9 km at Ri = .01 to 0.1 Km at Ri = .1 ; the corresponding figures for $(\lambda_o)_u$ are 4 Km and 0.2 Km.

In general for Ri between .2 and .3 the turbulence was weak and the spectral estimates fell to near noise levels, however some periods were observed in which the turbulence was markedly sporadic (ie distinct bursts occurred lasting usually from $\frac{1}{2}$ - 4 minutes) and Ri varied between .2 and .7. For the latter case the high frequency fall off for temperature was greater than $n^{-\frac{2}{3}}$ (approx. $n^{-.8}$) whilst in the former case it was less (approx. $n^{-.5}$), see Fig 5 (a) and (b) (these conclusions should be compared with previous results from Okamoto and Webb (1970) who found that for Ri $>$ .2 some runs produced near zero slope whilst others gave slopes between - 1.2 and -2.5). In periods of weak turbulence the u spectrum was poorly defined but in the sporadic cases a slope at high frequency of $n^{-\frac{2}{3}}$ was maintained (see Fig 5(c)) and this permitted presentation of the spectrum in nondimensional form (see Fig (6)). For this data the average Ri and $(f_o)_u$ were .24 and .08 respectively.

It was interesting to enquire to what extent the spectral forms deduced from the 8m data might be applicable at higher levels in the boundary layer ie 46 and 91m. Examination of the various spectra available showed that organisation of the data in nondimensional form was not possible for u and T components since an $n^{-\frac{2}{3}}$ fall off was not apparent or a spectral gap was not discernible or the spectra were so scattered as to render any average curve meaningless. For the vertical velocity component however, in some periods, a comparison was possible and this is given in Fig (7). The measure of agreement is impressive, with equation (2) and A = .146 providing a good representation of the spectra.

4. <u>Cospectral characteristics of the turbulence subrange</u>:-

During the night 8/9 November 1972 the turbulent fluxes increased in response to synoptic scale developments which reach the Cardington area by early morning. This is illustrated in Fig (8) which shows the evolution of the vertical heat flux cospectra (at 8m) with time. For segments 1 to 3 the turbulence was weak (spectral estimates at high frequency near noise level) whilst during 4 and 5 it became sporadic (the traces exhibited a marked bursting nature), finally in segments 6 to 9 the turbulence was continuous and the spectra were fairly well defined. Figure (9) shows a uT cospectrum at 8m plotted in logarithmic form (as noted by Kaimal (1973) the slope at high frequency is better represented by an $n^{-3/2}$ line rather than the n^{-2} slope predicted by Wyngaard and Cote (1972)). The spectral gap appears rather broad and 'u' - shaped which renders the choice of a lower frequency limit somewhat subjective, however it is clear that the first significant deviation from an n^{+1} roll off occurs near .008 Hz. For this reason and for consistency with the power spectral analysis the covariances were computed for the frequency interval $.008 < n < .5$ Hz.

When plotted in nondimensional form versus f/f_o the cospectra for stress, horizontal and vertical heat flux at 8m are well represented by the universal curves given by Kaimal (1973) (see Fig 10). The observed values for the f_o's were,

$(f_o)_{uw} = .22 \qquad (f_o)_{wT} = .33 \qquad (f_o)_{uT} = .14$

and with a Richardson number of .06 these are in good agreement with the values expected from Kaimal's relationships ie .19, .34 and .12 respectively. Comparison of the cospectra at 46 and 91m with the surface layer universal forms was not possible because a spectral gap was not identifiable and all the cospectral plots contained spectral estimates of both positive and negative sign

Concluding Comments:-

Turbulence spectra and cospectra at 8m obtained in stable conditions over the rather inhomogeneous and rough site at Cardington have been found to agree with the universal forms derived by Kaimal (1973) from data collected over a flat and uniform site in Kansas. The linear variation of the scaling parameter (f_o) for horizontal wind and temperature with Richardson number has been shown valid down to Ri values near.005. It was also demonstrated that on some occasions the spectral shape for the W component at 46 and 91m agreed with the surface layer form.

The significance of the low frequency spectral region was found to vary from one occasion to another but any spectral peaks that did occur were in the neighbourhood of the Brunt-Vaisala frequency. Further series of multilevel measurements are required to investigate the spectral forms at higher levels in the boundary layer and to determine the difference between spectra from levels within a nocturnal inversion to those from levels above it.

Acknowledgements:-

The author is indebted to the staff of the Meteorological Research Unit, Cardington and in particular to Miss S H Moss who carried out a preliminary analysis of the data.

TABLE 1

Height (m) (Z)	BRUNT-VAISALA FREQUENCY N(Hz)	$f_N = \frac{NZ}{u}$
8	.00107	.0026
46	.0008	.0045
91	.0007	.0080

LIST OF FIGURES

(c) :- Power spectrum for the horizontal wind component obtained during periods of sporadic turbulence.

Figure 6 :- Comparison between the nondimensionalized power spectra for horizontal wind speed for sporadic turbulence cases (plotted versus f/f_o) and the line (shown dashed)

$$\frac{n S_u(n)}{\overline{u^2}} = \frac{A(f/f_o)}{1 + A(f/f_o)^{5/3}}$$

with A = .3

Figure 7 :- Four nondimensionalized vertical velocity spectra (from 10/11 Jan.) at 46 and 91m plotted versus f/f_o. The dashed line represents the relation

$$\frac{n S_w(n)}{\overline{w^2}} = \frac{.164(f/f_o)}{1 + .164(f/f_o)^{5/3}}$$

Figure 8 :- Variation with time of the vertical heat flux cospectrum at 8m during the night 8/9 November 1972.

Figure 9 :- Cospectrum of the horizontal heat flux at 8m during periods of continuous turbulence.

Figure 10 :- Nondimensionalized cospectra plotted versus f/f_o compared to the universal curves from Kaimal (1973).

$$\frac{n S_{\alpha\beta}(n)}{\overline{\alpha\beta}} = \frac{0.88(f/f_o)}{1 + 1.5(f/f_o)^{2.1}}$$

and $\overline{\alpha\beta} = \overline{w\theta}, \overline{uw}$

$$\frac{n S_{\alpha\beta}(n)}{\overline{\alpha\beta}} = \frac{0.85(f/f_o)}{1 + 1.7(f/f_o)^{2.2}}$$

$$\overline{\alpha\beta} = \overline{u\theta}$$

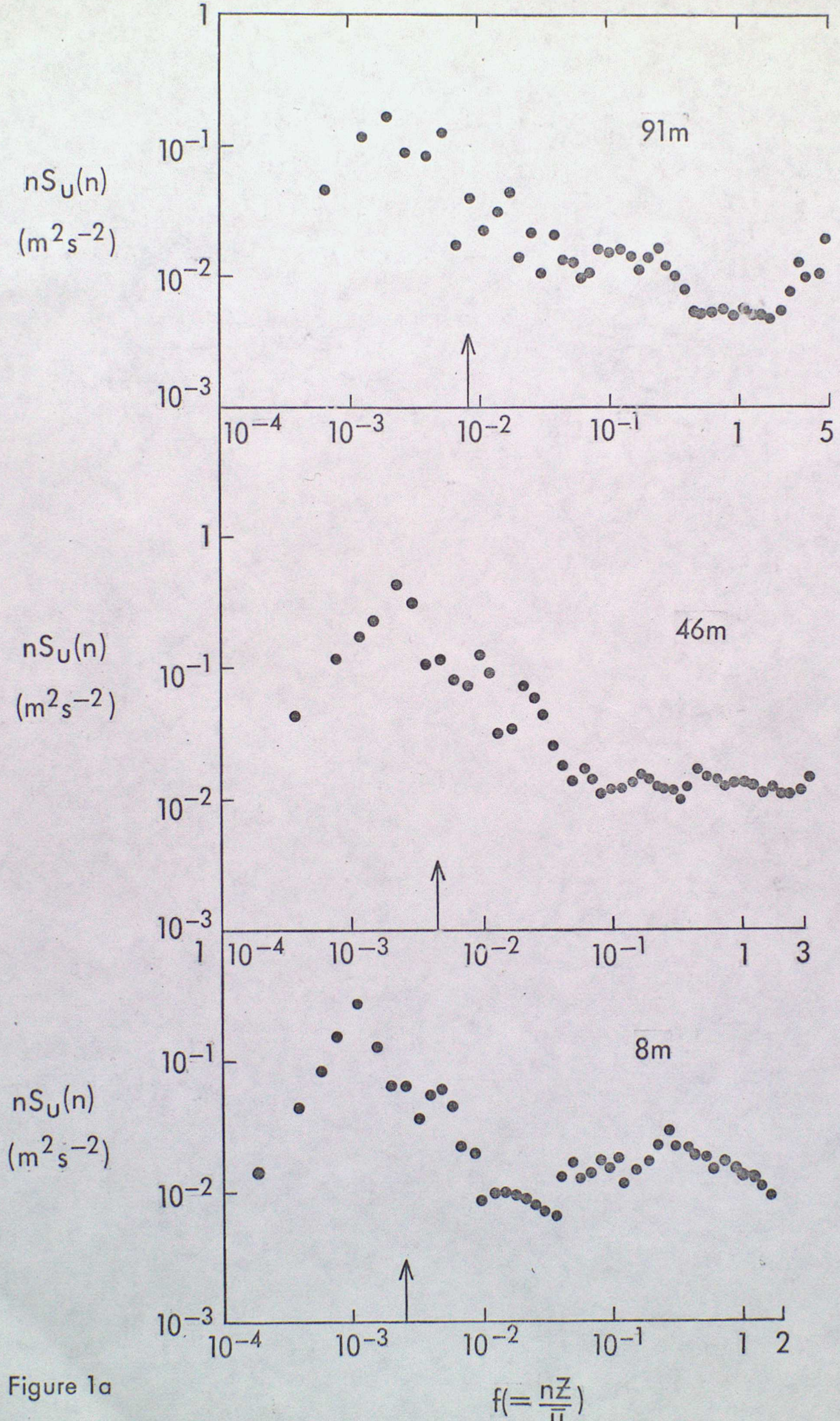

Figure 1a

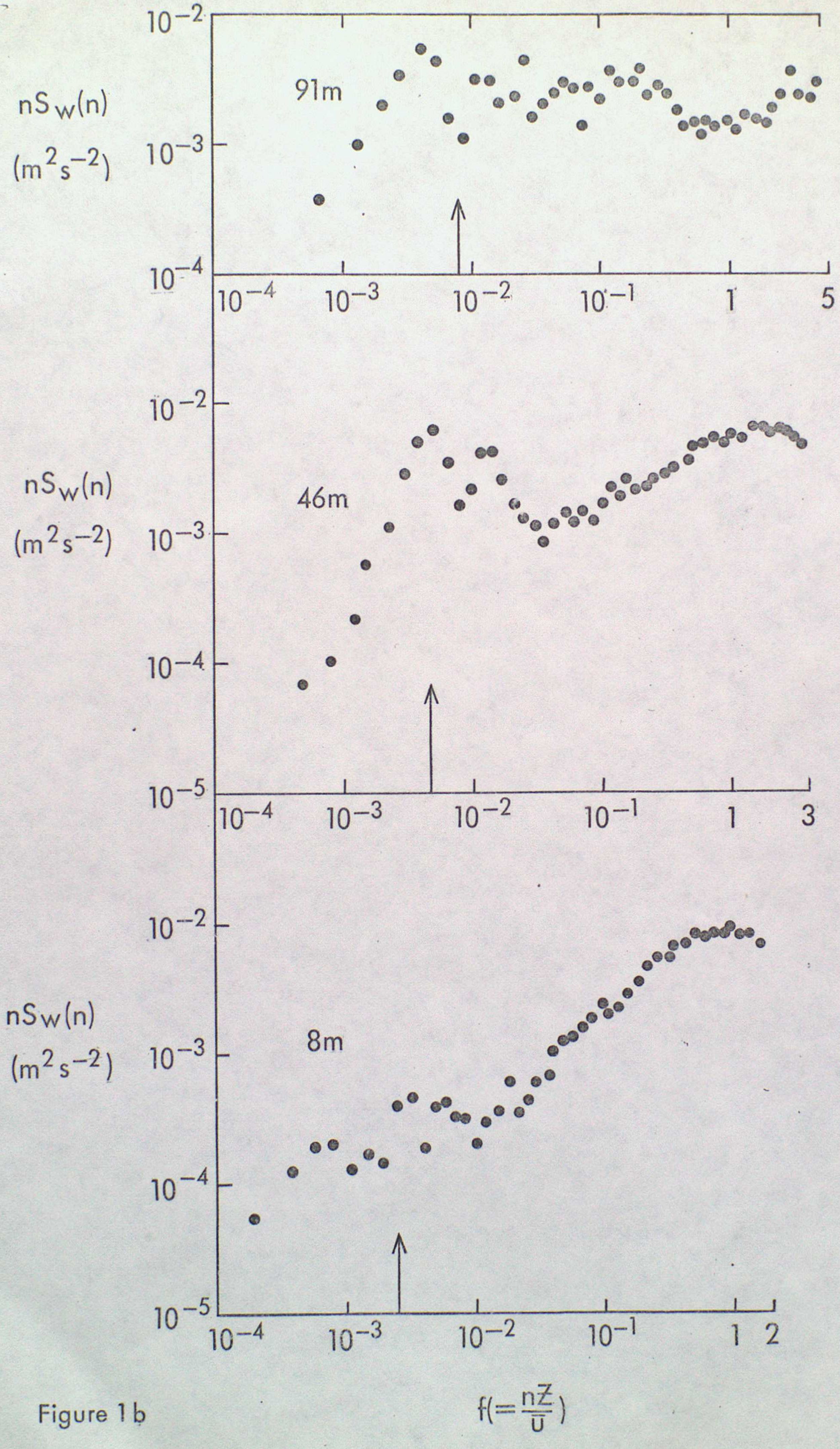

nSw(n)
(m2s-2)
91m
10-2
10-3
10-4
10-4
10-3
10-2
10-1
1
5
nSw(n)
(m2s-2)
46m
10-2
10-3
10-4
10-5
10-4
10-3
10-2
10-1
1
3
nSw(n)
(m2s-2)
8m
10-2
10-3
10-4
10-5
10-4
10-3
10-2
10-1
1
2
f(=nZ/U)

Figure 1b

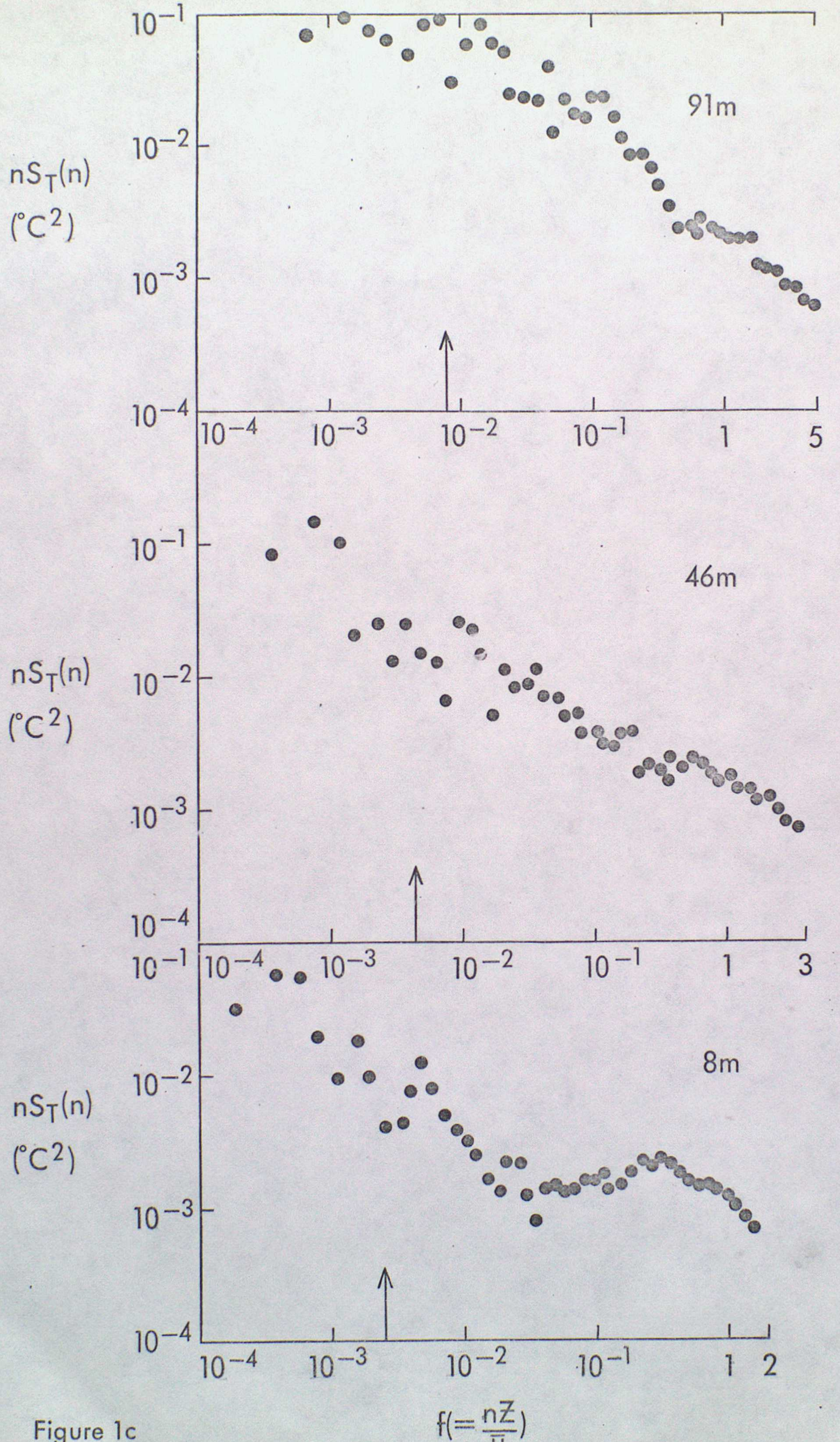

91m
46m
8m
nS_T(n)
(°C²)
10⁻¹
10⁻²
10⁻³
10⁻⁴
10⁻⁴ 10⁻³ 10⁻² 10⁻¹ 1 5
10⁻⁴ 10⁻³ 10⁻² 10⁻¹ 1 3
10⁻⁴ 10⁻³ 10⁻² 10⁻¹ 1 2
f(= nZ/ū)

Figure 1c

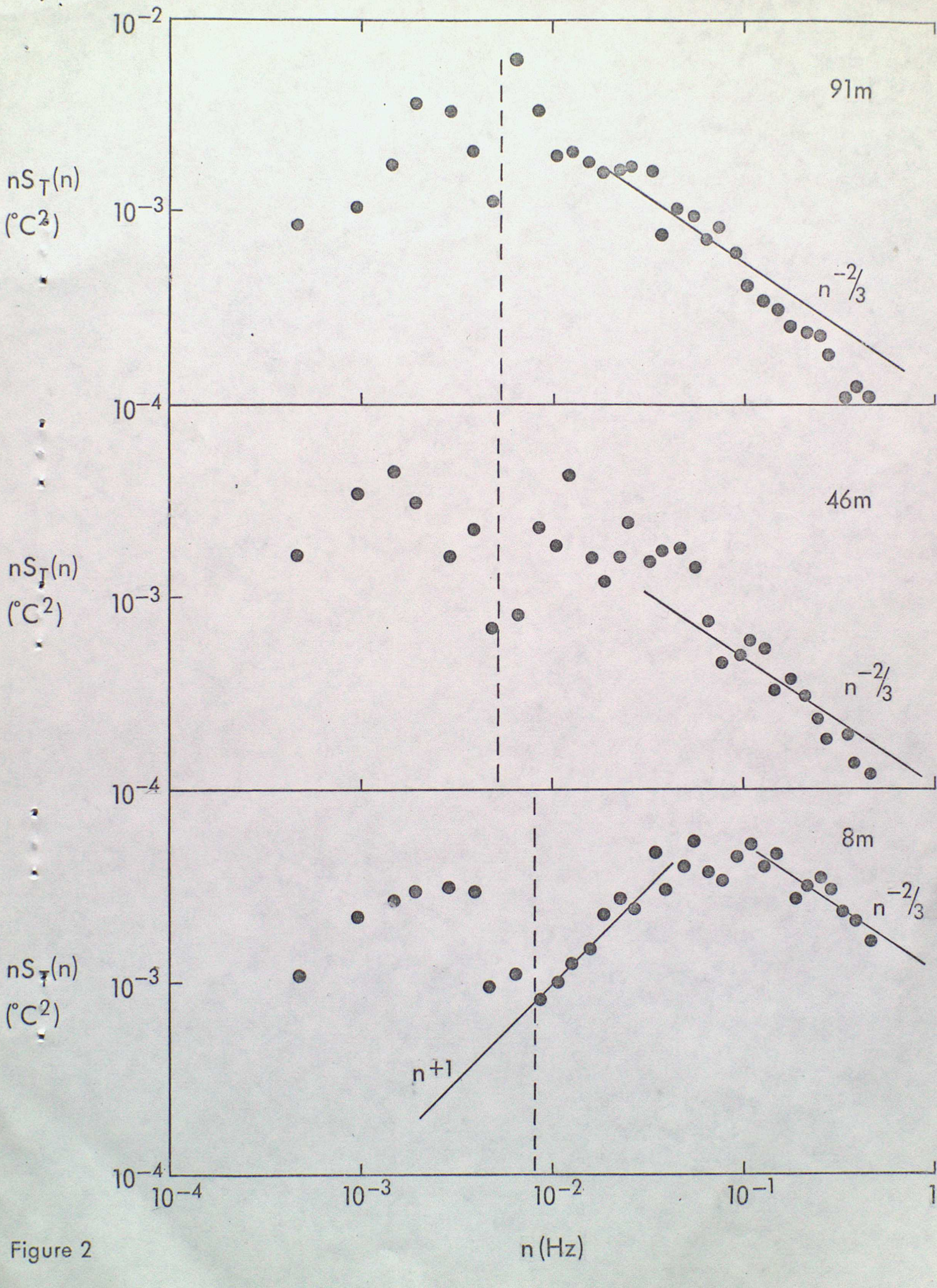

10⁻²
91m
nS_T(n)
(°C²)
10⁻³
n^-2/3
10⁻⁴
46m
nS_T(n)
(°C²)
10⁻³
n^-2/3
10⁻⁴
8m
n^-2/3
nS_T(n)
(°C²)
10⁻³
n^+1
10⁻⁴
10⁻⁴
10⁻³
10⁻²
10⁻¹
1
n (Hz)

Figure 2

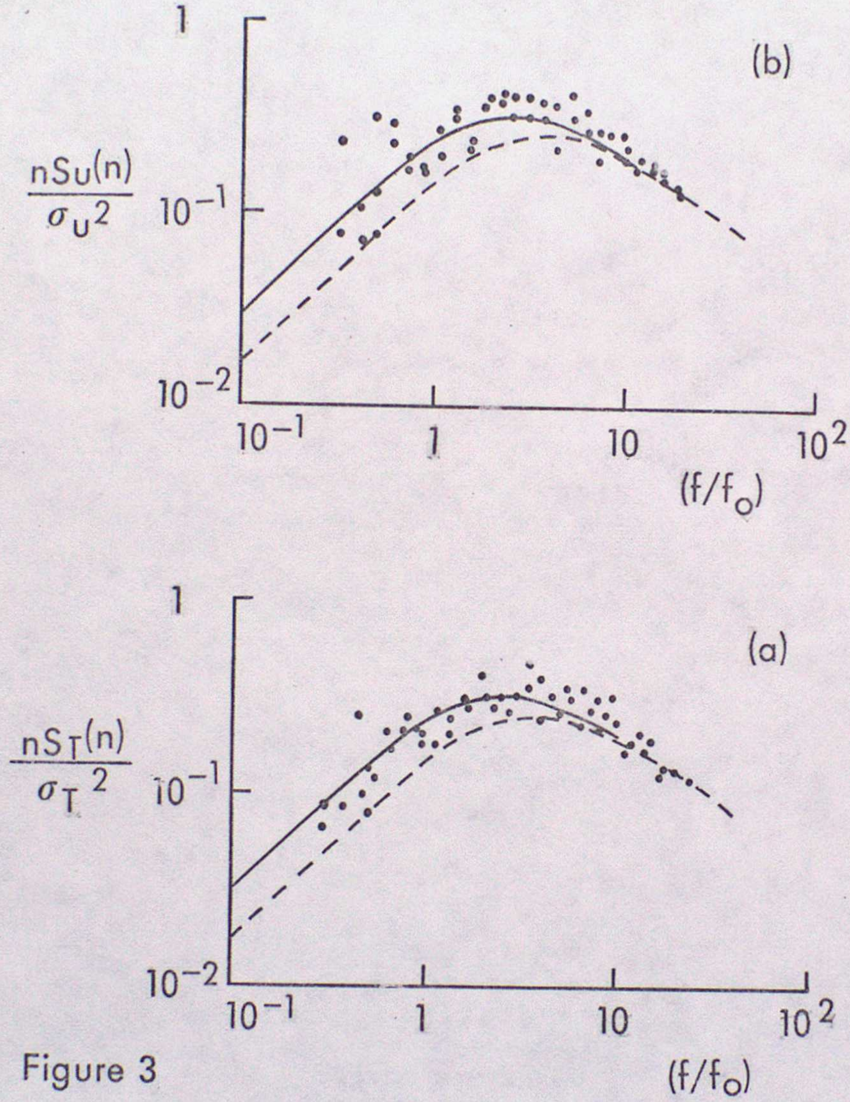
(b)
nSu(n) / σu²
1
10⁻¹
10⁻²
10⁻¹
1
10
10²
(f/fo)
(a)
nST(n) / σT²
1
10⁻¹
10⁻²
10⁻¹
1
10
10²
(f/fo)

Figure 3

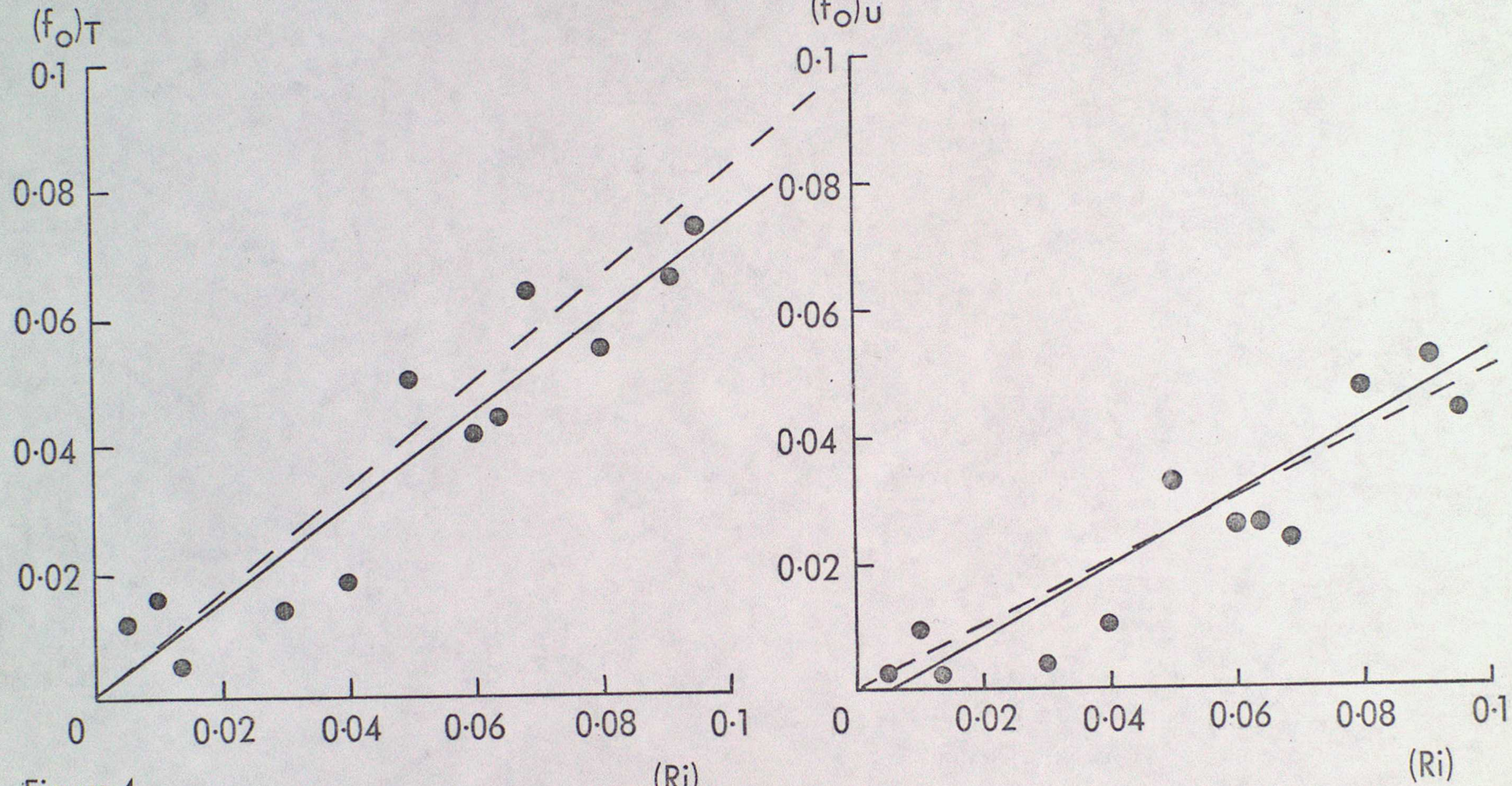

(fo)T
0·1
0·08
0·06
0·04
0·02
0
0·02
0·04
0·06
0·08
0·1
(Ri)
(fo)u
0·1
0·08
0·06
0·04
0·02
0
0·02
0·04
0·06
0·08
0·1
(Ri)

Figure 4

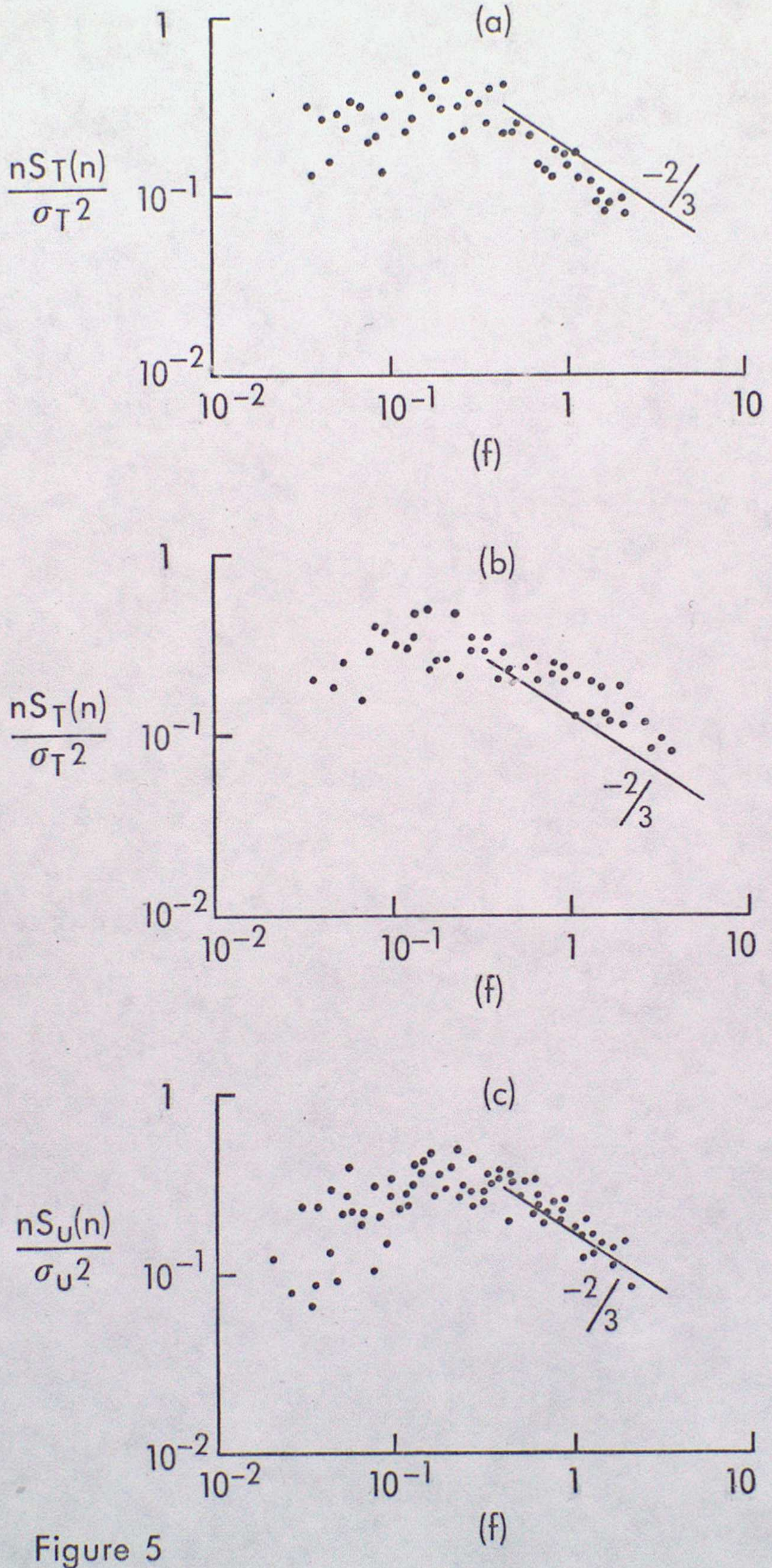
(a)
$\frac{nS_T(n)}{\sigma_T^2}$
1
10^{-1}
10^{-2}
10^{-2}
10^{-1}
1
10
(f)
$-2/3$
(b)
$\frac{nS_T(n)}{\sigma_T^2}$
(c)
$\frac{nS_u(n)}{\sigma_u^2}$

Figure 5

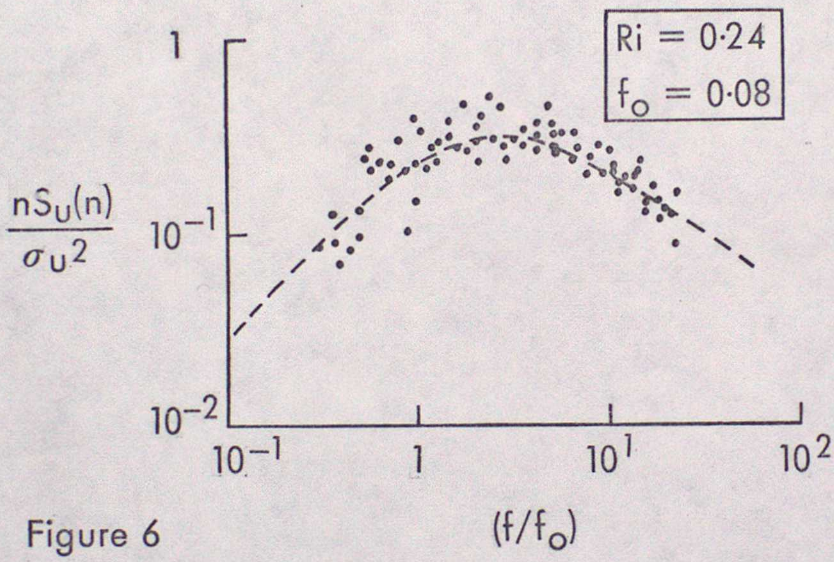

Figure 6

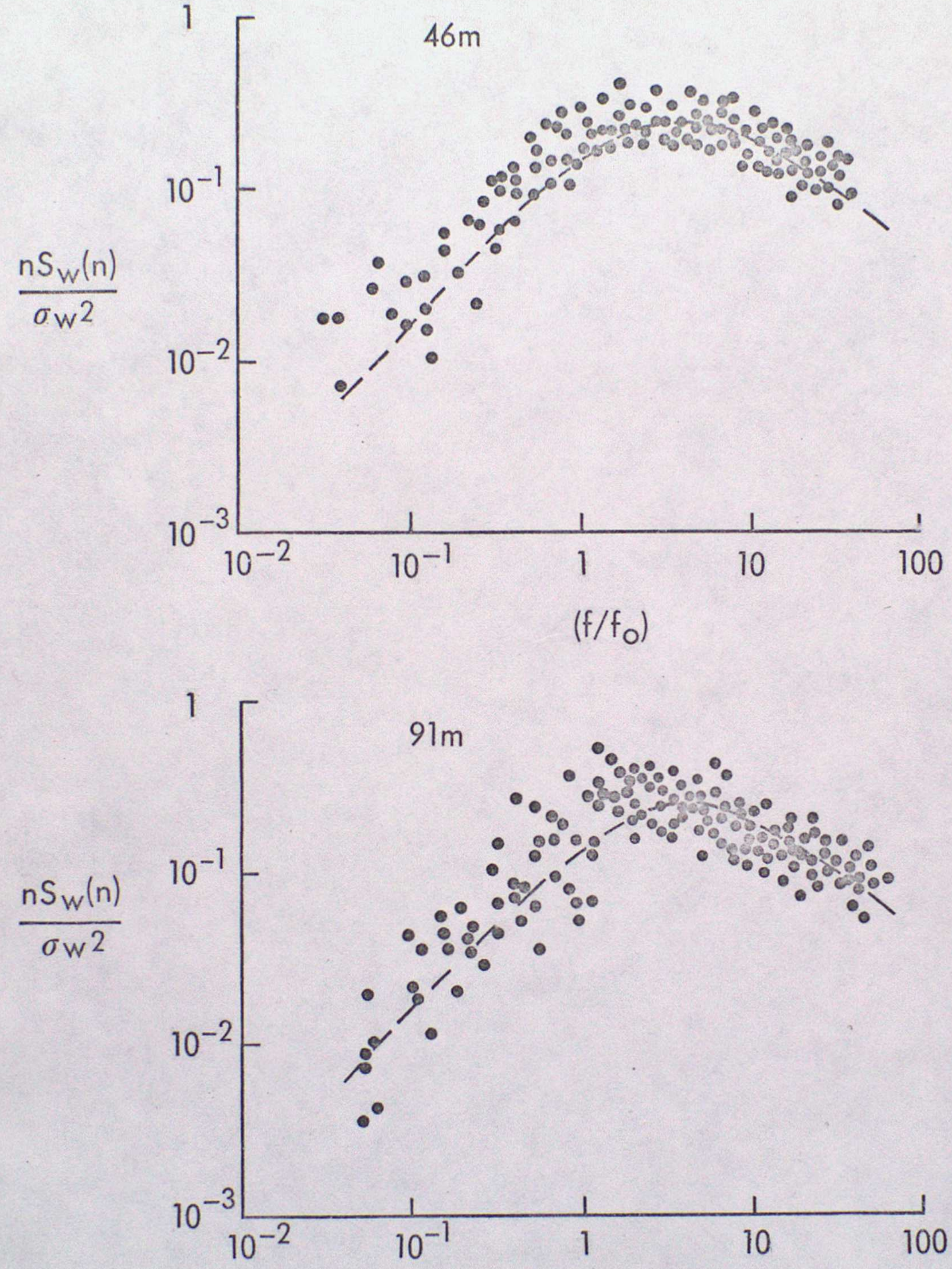
46m
nSw(n) / σw2
1
10−1
10−2
10−3
10−2
10−1
1
10
100
(f/fo)
91m
nSw(n) / σw2
1
10−1
10−2
10−3
10−2
10−1
1
10
100
(f/fo)

Figure 7

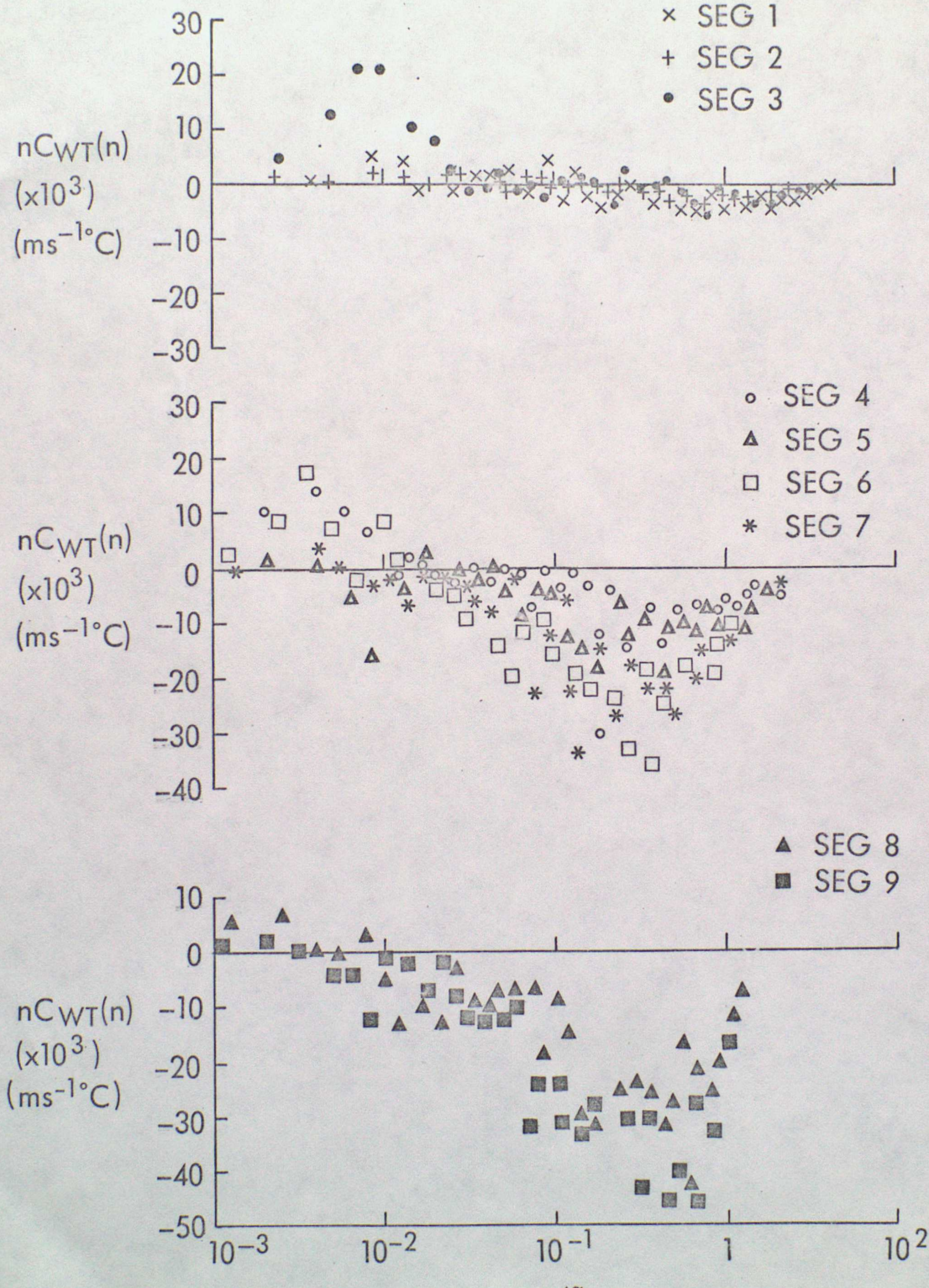
× SEG 1
+ SEG 2
• SEG 3
nCWT(n)
(x10³)
(ms⁻¹°C)
30
20
10
0
−10
−20
−30
○ SEG 4
▲ SEG 5
□ SEG 6
* SEG 7
−40
▲ SEG 8
■ SEG 9
−50
10⁻³
10⁻²
10⁻¹
1
10²
(f)

Figure 8

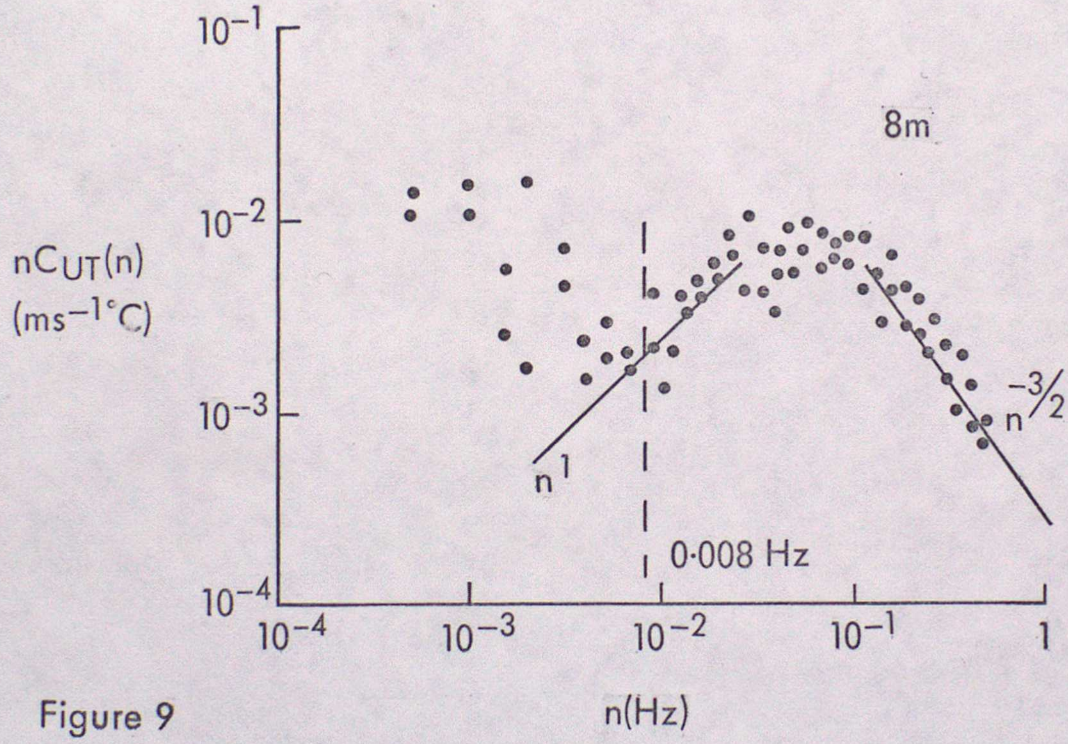

10⁻¹
10⁻²
10⁻³
10⁻⁴
nC_UT(n)
(ms⁻¹°C)
8m
n¹
n^-3/2
0·008 Hz
10⁻⁴
10⁻³
10⁻²
10⁻¹
1
n(Hz)

Figure 9

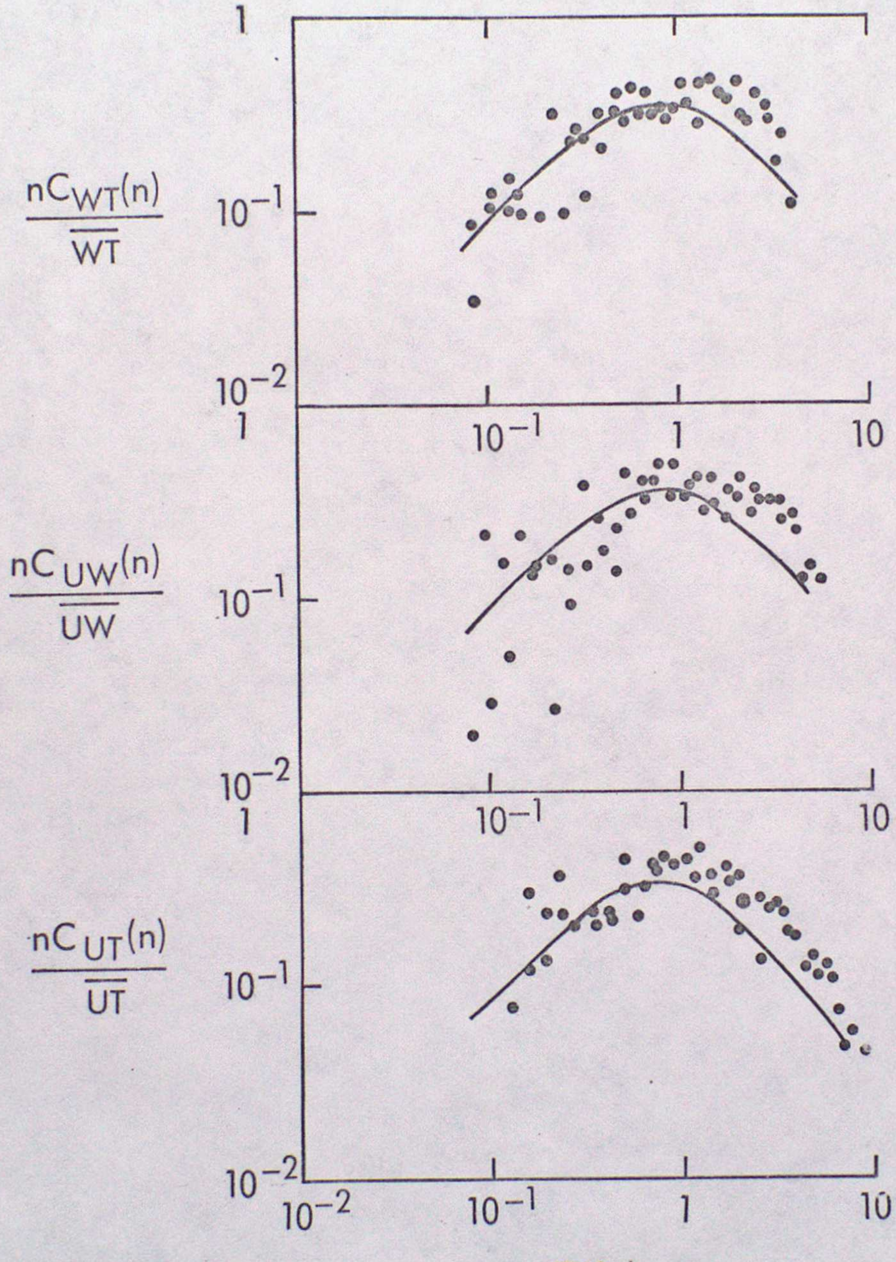

Figure 10